Seismic Risks Mitigation of Façadism Constructions with Supplemental Energy Dissipation

Ricky W. K. Chan[1*], Shilin Wang[2], Waiching Tang[3]

1 School of Engineering, RMIT University, Australia, ricky.chan@rmit.edu.au
2 Faculty of Architecture, Building and Planning, University of Melbourne, Australia
3 School of Architecture and Built Environment, The University of Newcastle, Australia

Abstract

Urban renewal projects involve redevelopments of under-utilised old buildings and revitalisation of precious land resources. Due to architectural and social-economic reasons, historical façades are sometimes retained, and new constructions are built behind them. This allows the historical façade, typically the street elevation, to remain while new real estate can be developed. In the profession of architecture, this is called façadism. In many cases, these historical façades are constructed with unreinforced masonry (URM). During demolition and construction, a temporary shoring retention frame is required prior to permanent connection to the new construction. These historical façades were made of brittle materials and were constructed many decades ago before modern design standards and materials were available. They possess little ductility and become vulnerable when subjected to ground shaking. Typically, the retained façades are treated as non-structural components and little attention is paid to their seismic performance. While most prior studies focus on strengthening of masonry or improving connection robustness between façades and the main structure, the present study attempts to take a different approach by limiting displacement demand on the façade. A new structural form is suggested which divides the new construction into two separate frames. A seismic gap is introduced between them and produces two structures of different vibrational characteristics. Supplemental energy dissipating devices such as viscous fluid or friction dampers are placed in-between adjacent floors. The façade is attached to a frame with smaller seismic mass and higher stiffness, while the second frame will undergo larger displacements in an event of ground shaking. In this manner, full advantage of supplementary energy dissipation is utilised, while protecting the façade from excessive displacements. In this article, governing equations are presented, followed by numerical simulations using historical earthquake acceleration histories. Results demonstrate that the suggested structural form is an effective methodology to suppress seismic responses of the façade and the new construction. It is concluded that damage on the retained façades can be prevented, and at the same time seismic responses to the newly constructed structure can be controlled.

Keywords

unreinforced masonry, facadism, heritage conservation, seismic risks mitigation, passive energy dissipation

10.7480/jfde.2021.2.4986

1 INTRODUCTION

1.1 FAÇADISM CONSTRUCTIONS

Population growths and continued urbanisation in many metropolitan cities and towns around the globe has put pressure on urban renewals. Often, heritage buildings are situated in locations with significant land value, but the original building construction diminishes the economic return for the property owners. Reuse or revitalisation of heritage buildings is very common, particularly throughout major cities. The strategy of retaining the street elevation façades of heritage buildings, while the main structures are demolished and rebuilt with modern design, has generated large interest. In the profession of architecture this is called façadism (Darley, 2015). When the rest of the building is demolished, the façade becomes a free-standing wall which may be unsafe to the public. Thus, a temporary shoring retention frame is required to provide lateral support and stability.

a b c d

FIG. 1 Examples of façadism in Melbourne, Australia

Figure 1(a) shows a new residential apartment development near Melbourne CBD, Australia. A historical masonry façade is retained while a reinforced concrete shear wall building is constructed behind it. Notice that the temporary shoring retention frame is built in front of the façade, occupying the pedestrian footpath. Figure 1(b) shows that an extensive shoring retention frame has been constructed while basement excavation works are in progress.

Figure 1(c) and (d) show completed façadism projects. The retained façade is connected to the new construction using tie rods, brackets, and anchor bolts. Although façadism is a controversial approach in architecture (Bullen & Love, 2011), this form of construction is increasingly common. Some consider the retention of historical façades to be an excellent initiative to preserve parts of history of an evolving built environment. In addition, a recent study (Tam et al., 2018) conducted in Australia compared life-cycle costs, which included heating and cooling energy consumption of eleven different façade systems. The study concluded that masonry façade performed the best.

1.2 SEISMIC RISK MITIGATION OF MASONRY STRUCTURES

Unreinforced masonry (URM) structures are considered seismically vulnerable due to their brittleness. Both masonry units and the mortar holding them together lack deformation capacity. In the 2010 and 2011 New Zealand Christchurch earthquakes, many unreinforced masonry and stone structures suffered severe damage, collapsed, and caused numerous fatalities (Ingham & Griffith, 2010; Ingham et al., 2011; Senaldi et al., 2014). Due to European settlements, the same type of unreinforced masonry construction is also commonly found in Australia, U.S.A., and Canada. An ample amount of research has been undertaken to assess vulnerability and seismic risk mitigations to masonry structures. The Federal Emergency Management Agency (FEMA) of USA summarised the historical damage to such structures in the U.S.A. and developed a risk reduction programme for existing structures in FEMA P-774 Reitherman and Perry (2009); Ferreira et al. (2010a); and Ferreira et al. (2010b) reported an extensive seismic assessment of 600 masonry façades in Portugal. Shake table test investigations (Candeias et al., 2017) and various simulation methods have been studied (Abdulla et al., 2017; Alshawa et al., 2017; Chácara et al., 2017; Derakhshan et al., 2017). The retrofitting of masonry structures using various strategies has been widely researched, for example by adding steel strips (Taghdi et al., 2000), synthetic mesh (Figueiredo et al., 2013), post-tensioning of supporting reinforced concrete frames (Soltanzadeh et al., 2018) and fibre-reinforced polymers (Triantafillou, 2001). Due to high seismicity in Italy, some seismic retrofit measures to masonry structures are reported (Mariangela De et al., 2018; Tiziana & Daniele, 2018). An extensive review on connections between historic masonry walls and horizontal diaphragms is presented by Solarino et al. (2019).

1.3 SEISMIC RISK MITIGATION OF PRECAST FAÇADES

Precast concrete façades or cladding units gained popularity in architecture as they provide an economical solution to the aesthetic appearance of the external faces of buildings. These panels are modular units which are usually supported on the face of buildings using steel brackets and bolts. In past earthquakes, severe damage to building façades has attracted much attention. In the 1980s, a systematic review of seismic risks to precast panels and cladding was conducted in the U.S.A., which comprised a review of the performance of the panels in past earthquakes, design and detailing rules, as well as the experimental testing of sample panels (Rihal, 1988). Similar studies continue to the present day, such as the Safecladding campaign in Europe (Negro & Lamperti Tornaghi, 2017), resulting in better understanding of panel dynamics and better designs (Dal Lago et al., 2018). In a related study, investigations into using glazed curtain walls as tuned mass dampers were numerically studied to mitigate seismic and impact risks (Bedon & Amadio, 2017; 2018).

1.4 OBJECTIVES OF THIS STUDY

Façadism is widely discussed in architecture and façadism projects are very common. However, seismic-risk mitigation specific to façadism construction is rare in literature. In many situations, the retained façade is rigidly connected to the new construction, and little attention is paid to its seismic performance. Due to its very limited ductility, severe damage or even complete collapse of the retained masonry wall may occur in a moderate seismic event. As discussed in the section 1.3, previous studies focused on seismic assessments, strengthening, and connection details of masonry walls. This paper takes a different approach and presents a new structural form which attempts to limit displacement demands on the masonry façade, while allowing the new construction to undergo larger displacement. The structural form introduces a seismic gap between the frame which supports the façade and the rest of the building, resulting in two vibrating systems. Supplemental energy dissipating devices are incorporated within the seismic gap. The system utilises the principles of supplemental energy dissipation using designated devices, which have been widely studied and adopted (Soong & Costantinou, 2014; Symans et al., 2008) to connect two adjacent frames. Through the differences in vibrating velocities or displacements, energy is absorbed by the devices. In this manner, full advantage of supplementary energy dissipation is utilised, while protecting the façade from excessive displacement. The study begins with formulation of equation of motions with linear viscous fluid dampers and nonlinear friction dampers. It is followed by a numerical example with finite element modelling of a masonry façade and time domain analyses of the proposed system. Finally, insights drawn from numerical examples and issues concerning practical implementation are discussed.

2 PROPOSED STRUCTURAL FORM

2.1 GENERAL DESCRIPTION

A feasible structural form will need to fulfil the architectural requirement that a thin, street elevation façade wall is retained, while the complete structural form, including the façade and the new frame built behind it, withstands service wind loads and design earthquake loads. When the façade is retained and the remainder of the building is demolished, it becomes a free-standing wall and does not possess lateral stability. Current state-of-practice construction procedure involves the construction of a temporary steel shoring frame to provide structural stability during works, as shown in Figure 1(a) and (b).

To mitigate seismic risks, due to its inherent brittleness, the masonry façade must undergo small displacements under design earthquakes. The new construction, on the other hand, is built with modern materials and technology and may undergo larger displacements. A structural form with a seismic gap is proposed herein and presented in Figure 2. The new construction is divided into two structural frames. The façade wall is supported by a laterally stiff frame, Frame-B. Its high stiffness prevents the façade wall from excessive deformation under design earthquakes. Frame-B is physically separated from the rest of the building, denoted by Frame-A, by a seismic gap. Each adjacent level is connected by a supplemental energy-dissipating device. k represents the height of façade, while n represents the height of Frame-B. Frame-A is m levels higher than Frame-B.

The two frames will possess different vibrational characteristics. Under seismic action, relative movements between the two frames cause energy dissipation to occur in the devices, achieving the goal of vibration control.

2.2 CHARACTERISTICS AND ADVANTAGES OF PROPOSED STRUCTURAL FORM

The proposed structural form has the following distinct characteristics and advantages over traditional placements of supplemental energy dissipation devices on braces:

1. Partitioning the new construction allows the two frames to be designed and constructed to a different set of requirements. For example, high lateral stiffness is required for Frame-B and it can be constructed in reinforced concrete or braced steel frame. Frame-A can be constructed with less structural stiffness but larger ductility requirements. It adds flexibility and may result in potential cost-saving.
2. Horizontal placements of supplemental energy devices – the travels of devices equal to relative displacements between two adjacent levels. Unlike traditional placement of devices on a diagonal brace, device travel is reduced by cos$q$ (where q is angle of diagonal brace to horizontal). Installation of devices is also simpler.
3. The seismic gap within the building may impose space utilisation issues but it can be used as a space for vertical transportation of building services.

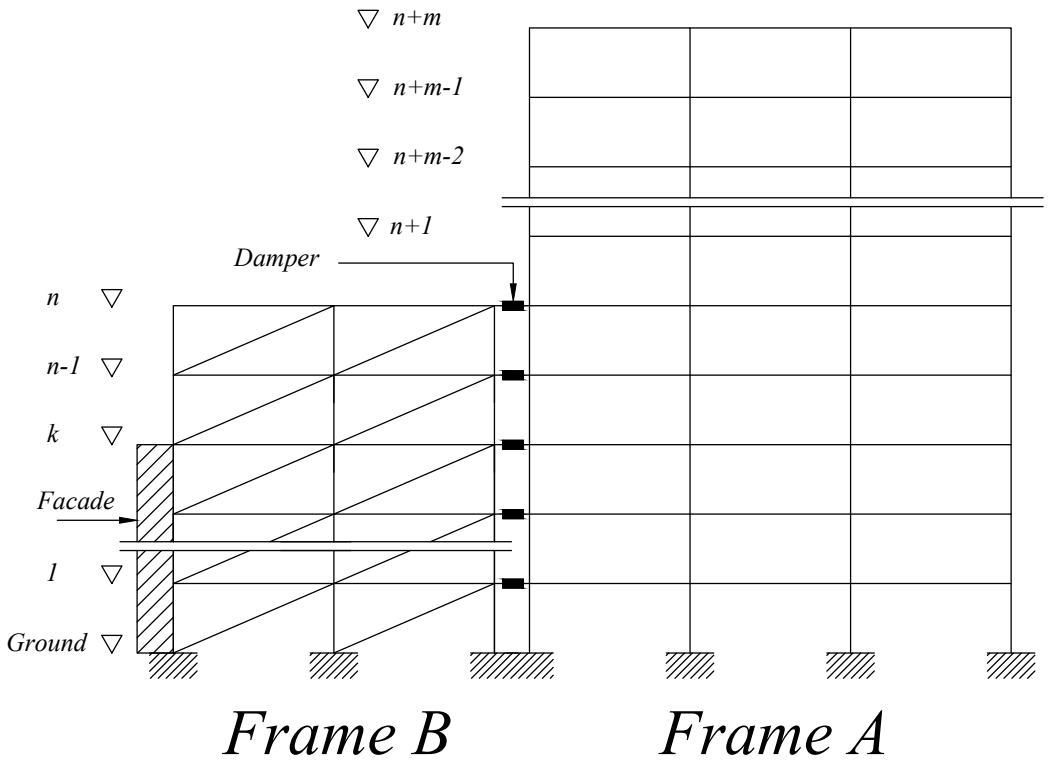

FIG. 2 Proposed structural form to retain historical façade

2.3 SYSTEM FORMULATION WITH LINEAR VISCOUS FLUID DAMPERS

Viscous fluid (VF) dampers first find applications in automotive, military, and aerospace engineering to suppress vibration problems. Nowadays, massive VF dampers are manufactured and widely used to suppress structural vibration due to earthquakes and winds in civil structures. VF dampers typically consist of a piston within a cylindrical housing filled with silicone or similar type of oil. When the piston is displaced, the viscous oil is forced through small orifices from one side to another (Constantinou & Symans, 1993; Reinhorn & Constantinou, 1995) within the housing, generating resilience force related to the velocity. The resilience force can be approximated by $f_d = c_d V^r$, and the exponent r typically ranges from 0.3 to 2.0. Modern dampers manufactured by Taylor Device Inc. have output force ratings up to 8900kN (2 million pounds) and amplitudes up to 1.06m (+/-42 inches) ("Taylor Devices Inc. Fluid Viscous Dampers"), while those manufactured by ITT Enidine Inc. have output force ratings up to 8896kN and amplitudes up to 1.52m (60 inches) ("IIT Enidine Inc. Viscous dampers / Seismic dampers"). Other manufacturers located in Europe and Japan are also available in the market. VF dampers are incorporated in thousands of buildings in earthquake-prone countries such as Japan (Nakamura & Okada, 2019), US (Symans et al., 2008) and Taiwan (Wang et al., 2017), and considered one of the most mature seismic risk mitigation technologies. Various design strategies have been developed, such as energy-based design (Habibi et al., 2013), target damping ratios, minimising inter-storey drifts, and minimising life-cycle costs. De Domenico et al. (2019) recently presented an overview on design strategies. Figure 3 shows a VF damper in a steel structure in Japan. VF dampers have several advantages, including their availability, reliability, and easy modelling due to their linearity (for velocity exponent of 1.0); they also produce 90 degrees phase difference with the elastic restoring force of structure and do not add significant stiffness to structural elements. However, their damping force is dependent on velocity and may not generate sufficient damping force regardless of the value of C_d. Therefore, their effectiveness must be thoroughly investigated under design earthquake time-histories.

FIG. 3 A viscous fluid (VF) damper manufactured by KYB Corporation, Japan

Through the introduction of a seismic gap, the structure is now divided into two vibrating systems. Its dynamic formulation is presented by Xu et al. (1999). Equation 1 represents the equation of motion of a dual multi-degree-of-freedom systems. M_A, K_A, and C_A represent the mass, stiffness, and

damping matrices of Frame-A. M_B, K_B, and C_B represent those of Frame-B. The mass, stiffness, and damping of the masonry façade are also included in formulation of Frame-B quantities. x represents the vector containing relative movement from ground, *t* is a vector of 1's and $\ddot{x}_g$ is a vector containing the acceleration of ground due to seismic actions. Assuming the floor levels of Frame-A and B are at the same elevations, each adjacent level is interconnected by VF dampers characterised by damper stiffness k_d and damper viscous damping c_d.

$$M_S\ddot{x} + C_s\dot{x} + K_s x = -M_s \tau \ddot{x}_g \tag{1}$$

where

$$M_s = \begin{bmatrix} M_A & 0 \\ 0 & M_B \end{bmatrix} \tag{2}$$

$$C_s = C_0 + C_c \tag{3}$$

$$C_0 = \begin{bmatrix} C_A & 0 \\ 0 & C_B \end{bmatrix} \tag{4}$$

$$C_c = \begin{bmatrix} C_d & 0 & -C_d \\ 0 & 0 & 0 \\ -C_d & 0 & C_d \end{bmatrix} \tag{5}$$

$$C_d = diag\left(c_{d1}\, c_{d2} \cdots c_{di} \ldots c_{dn}\right) \tag{6}$$

$$K_s = K_0 + K_c \tag{7}$$

$$K_0 = \begin{bmatrix} K_A & 0 \\ 0 & K_B \end{bmatrix} \tag{8}$$

$$K_c = \begin{bmatrix} K_d & 0 & -K_d \\ 0 & 0 & 0 \\ -K_d & 0 & K_d \end{bmatrix} \tag{9}$$

$$K_d = diag\left(k_{d1}\, k_{d2} \cdots k_{di} \ldots k_{dn}\right) \tag{10}$$

In Equation (6) and (10), c_{di} and k_{di} represent the damping coefficient and elastic stiffness of the i^{th} damper, respectively. As shown, two dynamic systems of Frame-A and B are coupled together in Equation (1). This equation is linear if the VF damper exponent *r* is assumed 1.0, and the main structural components are excited within their elastic limits.

2.4 SYSTEM FORMULATION WITH FRICTION DAMPERS

Friction dampers utilise frictional force developed between contacting surfaces as a means to dissipate input energy. If the conditions of contacting surfaces are kept consistent and normal forces are carefully controlled, friction dampers may generate force-displacement hysteresis repeatedly without strength degradation. Some designers consider friction dampers as a cost-effective alternative to VF dampers. They typically involve two or more contacting metal surfaces clamped together by a known normal force. The first author has fabricated and tested a linear-motion friction damper (Chan & Hu, 2016) similar to the Slot Bolted Connections (SBC) developed by Grigorian et al. (1993). The damper was fabricated with two short-length channel sections arranged back-to-back, with a 20mm thick steel shim sandwiched in-between. Long slots were cut in the channel sections which allowed the shim plate to slide in a guided motion. Two 16mm diameter structural bolts were pretensioned to a specified force. Normal force can be adjusted by varying tensions in connecting bolts, and the resultant frictional force provides a means of energy-dissipation during movements of the structure.

FIG. 4 Linear-motion friction damper (Chan & Hu, 2016)

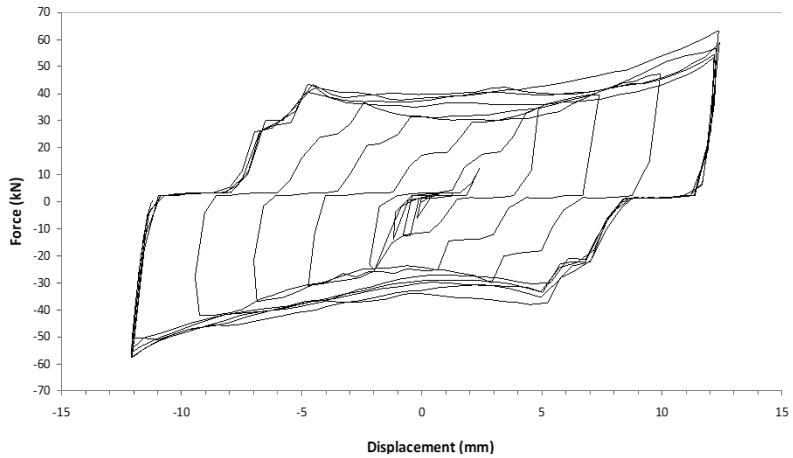

FIG. 5 Force-displacement characteristics of test specimen (Chan & Hu, 2016)

Figure 4 shows the tested specimen and Figure 5 shows the force-displacement hysteresis obtained with polished and cleaned surfaces (Chan & Hu, 2016). It can be seen that a 40kN capacity damper is produced by an approximately 5kg device. Friction dampers typically exhibit close-to "rigid-perfectly-plastic" behaviour and the Coulomb friction model may provide reasonable estimation. A friction damper of 5000kN capacity has been reported (Mualla et al., 2010) which involves multiple steel plates deforming in a rotational motion.

When friction dampers are used in the proposed structural form, the equations of motion will need to include the nonlinear frictional forces. For two multi-degree-of-freedom dynamic systems interconnected with friction devices, the equation of motion (Bhaskararao & Jangid, 2006) can be written as

$$M_s\ddot{x} + C_0\dot{x} + K_0 x = -M_s\tau\ddot{x}_g + F_D \tag{11}$$

where M_s, C_0 and K_0 have been defined previously, and the friction dampers' contribution in the equations of motion is defined by,

$$F_D^T = \left\{ \mathrm{f}_{d(n,1)} 0_{(m,1)} - \mathrm{f}_{d(n,1)} \right\} \tag{12}$$

$$\mathrm{f}_D^T = \left\{ f_{d1}, f_{d2,} \cdots, f_{di,} \cdots, f_{dn-1}, f_{dn} \right\} \tag{13}$$

In Equation (13), f_{di} is the i^{th} damper force. A common approach to simulate the nonlinear resilient behaviour of the friction dampers is the Bouc-Wen model (Wen, 1976). The Bouc-Wen model involves a first order differential equation which can be coupled with equation of motions. The model has found a wide range of applications including frictional behaviour in dampers (Bhaskararao & Jangid, 2006; Constantinou et al., 1990), metallic yielding dampers (Zhu & Lu, 2011) and semi-active magnetorheological dampers (Spencer et al., 1997). Here, the frictional force is multiplied by a hysteretic parameter *z*,

$$f_{di} = \mu N z \tag{14}$$

where μ is the coefficient of friction, *N* is the normal force generated by the bolt tension. *z* is a non-dimensional hysteretic component described by the following first-order differential equation,

$$\frac{dz}{dx} = A - \left[\beta + \gamma \,\mathrm{sgn}\left(\dot{x} z \right) \right] |z|^j \tag{15}$$

The shape of hysteresis can be tuned by non-dimensional parameters A, β, ɣ and *j*. In-depth discussion on the Bouc-Wen model is recently presented by Chang et al. (2016).

3 EVALUATION OF NUMERICAL EXAMPLES

3.1 EVALUATION MODEL

In this section the proposed structural form is evaluated using numerical examples based on typical façadism construction. The evaluation model consists of a 7.0m high, 450mm thick unreinforced masonry wall façade being retained in a new construction. The façade is characterised by 4x2 arch windows with dimensions shown in Figure 6(a). A new 6-storey steel structure is built behind it, as shown in Figure 6(b). The floor-to-floor height is 3.5m and the frames are spaced at 9.0m (into paper). The masonry façade is supported laterally by Frame-B which is a 5-storey, single-bay braced steel frame. Large steel sections are selected for Frame-B to provide large lateral stiffness to the façade. This frame is physically separated from the rest of the construction, Frame-A which is a 6-storey steel moment resisting frame. VF dampers are placed between the two frames on each adjacent level. Relative movements between the adjacent level will cause displacement (and velocity) within the VF dampers. The damper properties are assumed identical throughout. With reference to the notations described in Figure 2, $k = 2$; $n = 5$ and $m = 1$.

The numerical investigation also involves a comparison model, Frame-C, which represents a conventional construction without seismic gap or dampers, as shown in Figure 6(c). Frame-C has identical seismic mass, geometry, beam and column cross- sections, but there is no supplementary energy dissipating device or a seismic gap. Dynamic properties of the frames are listed in Table 1.

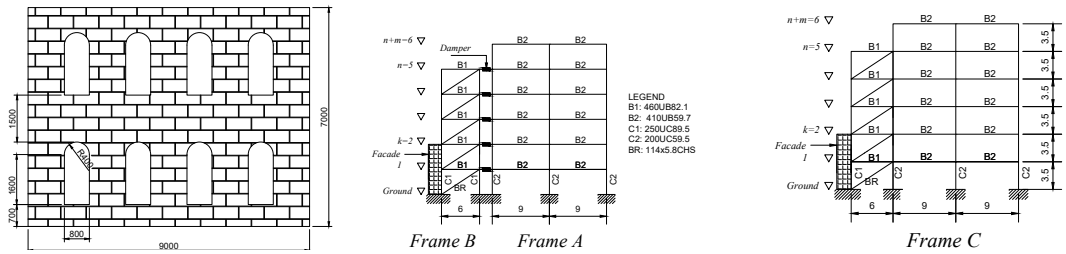

1 2 3

FIG. 6 Evaluation models in numerical example (a) façade dimensions, (b) proposed structural form and (c) comparison frame

TABLE 1 Frame properties

DESCRIPTION	FRAME A	FRAME B	FRAME C
Number of storeys	6	5	6
Storey mass [ton]	58.8 (Level 1-6)	49.3 (Level 1 &2)	108.2 (Level 1 &2)
	-	19.6 (Level 3-5)	78.4 (Level 3-5)
	-	-	58.8 (Level 6)
Total mass [ton]	352.8	157.4	510.4
Damping ratio z	2%	2%	2%
Period 1 [sec]	2.759	0.518	2.012
Period 2 [sec]	0.906	0.211	0.736
Period 3 [sec]	0.528	0.126	0.471

3.2 FINITE ELEMENT ANALYSIS OF MASONRY FAÇADE

A finite element (FE) analysis is conducted to determine the out-of-plane stiffness, elastic limit, and failure mode of the masonry façade. The commercial FE package Abaqus (version 2018) is used. A macro-modelling approach is adopted: the masonry façade is modelled as a homogenous material – the masonry units, mortar, and interface between them are represented by an equivalent continuum (Chácara et al., 2017). To capture the brittle material properties of masonry, the extended FEM approach (XFEM) (Moës et al., 1999) is applied to capture crack propagation. Meanwhile, traction separation law is used in XFEM to stimulate masonry units' crack initiation and propagation. Furthermore, the Drucker Prager plasticity model is applied. The Abaqus eight-node brick elements with reduced integration (C3D8R) are used. The masonry wall is assumed to be free-standing with fixed boundary conditions at its base, and the remaining three sides are free. Displacement is applied on the top of the façade. Material properties for the FE model are defined according to literature (Abdulla et al., 2017; Griffith & Vaculik, 2007) which were calibrated against experimental data, and summarised in Table 1.

TABLE 2 Material properties of unreinforced masonry FE model

DESCRIPTION	VALUE (GRIFFITH & VACULIK, 2007)
Elastic modulus	3540 MPa
Poisson's ratio	0.15
Tensile strength	1.18 MPa
Shear strength	1.65 MPa

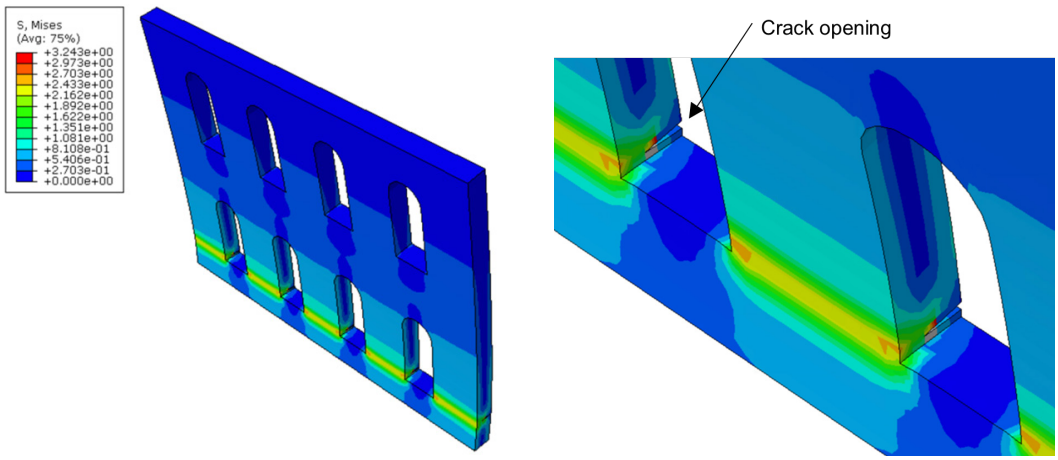

FIG. 7 FE analysis of masonry façade, (a) FE mesh, (b) von Mises stress, and (c) crack opening

Figure 7(a) depicts the von Mises stress at the end of analysis (top displacement =38.0mm). It is clear that the stresses are concentrated near the bottom of the window openings where the façade is weakened by the openings. With the aid of XFEM modelling, cracks caused by tension are clearly visible at the back of the façade (Figure 7b). Figure 8 depicts the load-displacement curve of the FE analysis. Displacement is measured at the top of façade. The façade behaves linearly until its elastic limit is reached at 33.1mm displacement (rotation f = 4.4x10^{-3} rad). Thereafter, the stiffness and strength degrade rapidly and the façade fails. Measured from this curve, the out-of-plane elastic stiffness is 1.43kN/mm - a small value compared to those of steel frames. It can be concluded

that the façade wall fails in a brittle manner and failure is caused by tension cracks near the discontinuity (window openings).

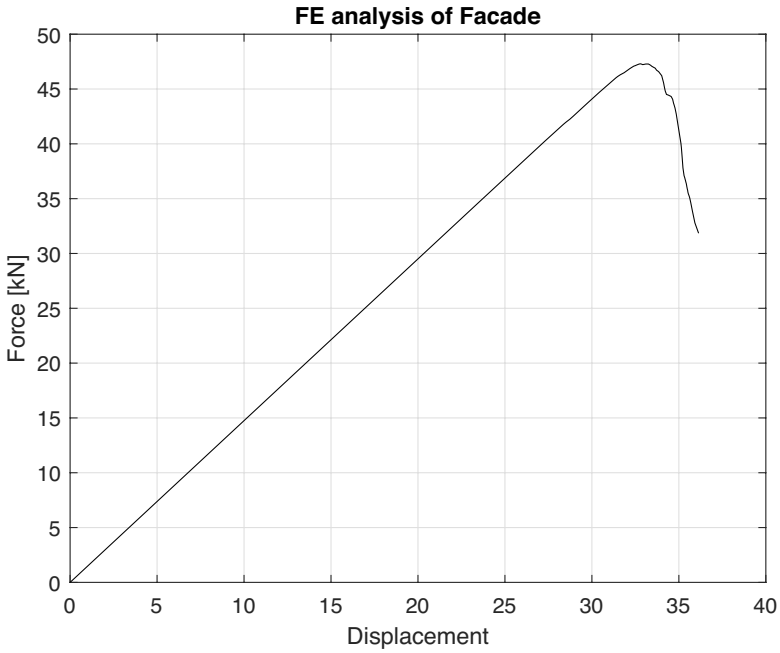

FIG. 8 Force-displacement curve of FE analysis of masonry façade

3.3 PERFORMANCE WITH LINEAR VISCOUS FLUID DAMPERS

Four historical strong earthquakes are used to evaluate the structural performance of the system. The four earthquake histories are recommended as benchmark problems for structural control (Ohtori et al., 2004), which consist of two near-field and two far-field records: (1) El Centro, the N—S components recorded at the Imperial Irrigation District substation in El Centro California during the Imperial Valley California Earthquake on 18th May 1940; (2) Hachinohe: the N-S component recorded at Hachinohe City during the Tokachi-oki earthquake on 16th May 1968; (3) Northridge, the N-S component recorded at Sylmar County Hospital during the Northridge California earthquake on 17th January 1994; and (4) Kobe, the N-S component recorded by Japanese Meteorological Agency during the Hyogoken-Nanbu earthquake on 17th January 1995. Their absolute peak accelerations are 0.348g, 0.229g, 0.843g and 0.834g, respectively.

Numerical models with properties listed in Table 1 are developed in MATLAB. The façade wall is attached to Frame B. The façade contributes its mass to the seismic mass of Frame B. Its FE modelling—described in the last section—showed that its lateral stiffness is small and thus neglected. The damping matrices are formulated using Rayleigh mass and stiffness proportional damping with the first two modes equal to 2%. VF dampers are assumed identical throughout the height with $k_d = 0$ and $c_d = 1000kNs/m$. The dynamic system is modelled with the state-space approach and the time response to one-dimensional ground motions are simulated using the MATLAB commend *lsim*.

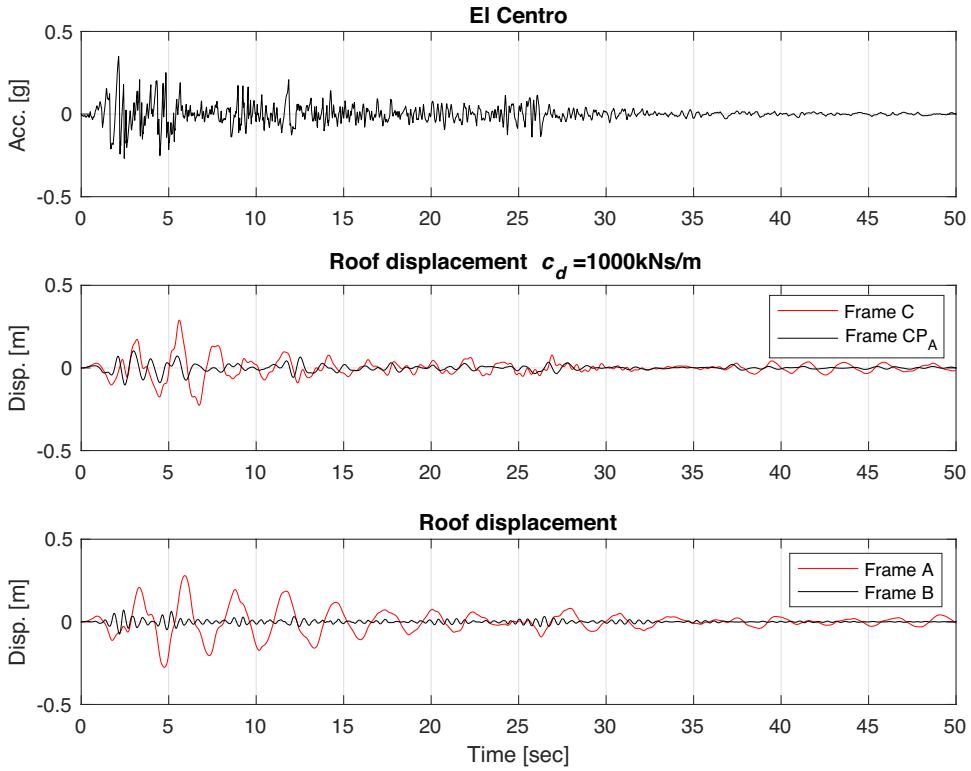

a *El Centro Earthquake*

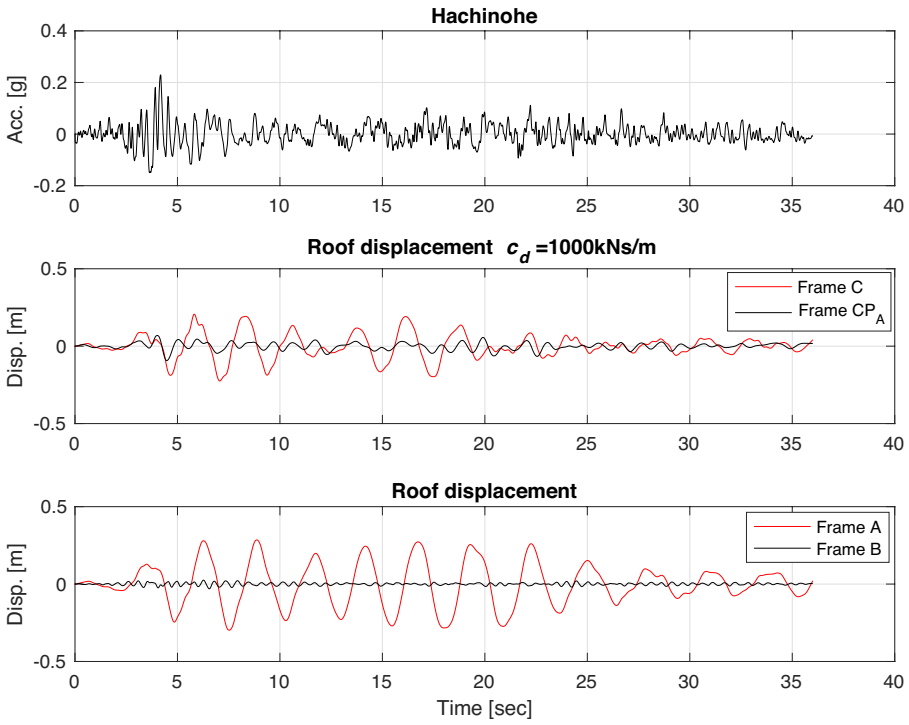

b *Hochinohe Earthquake*

FIG. 9 Roof level displacement time histories (VF dampers)

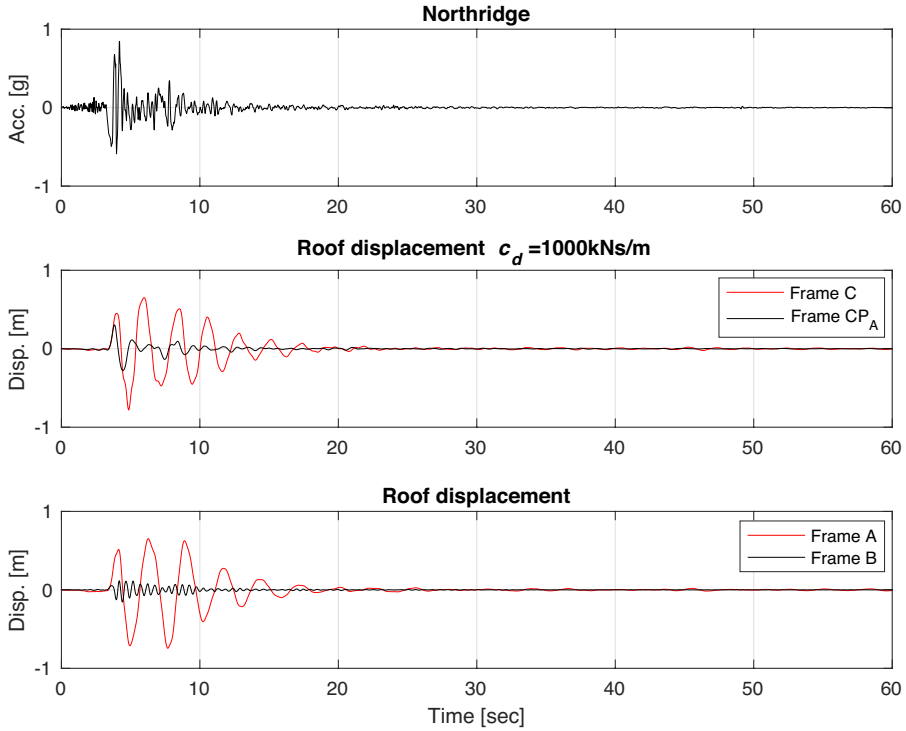

c *Northridge Earthquake*

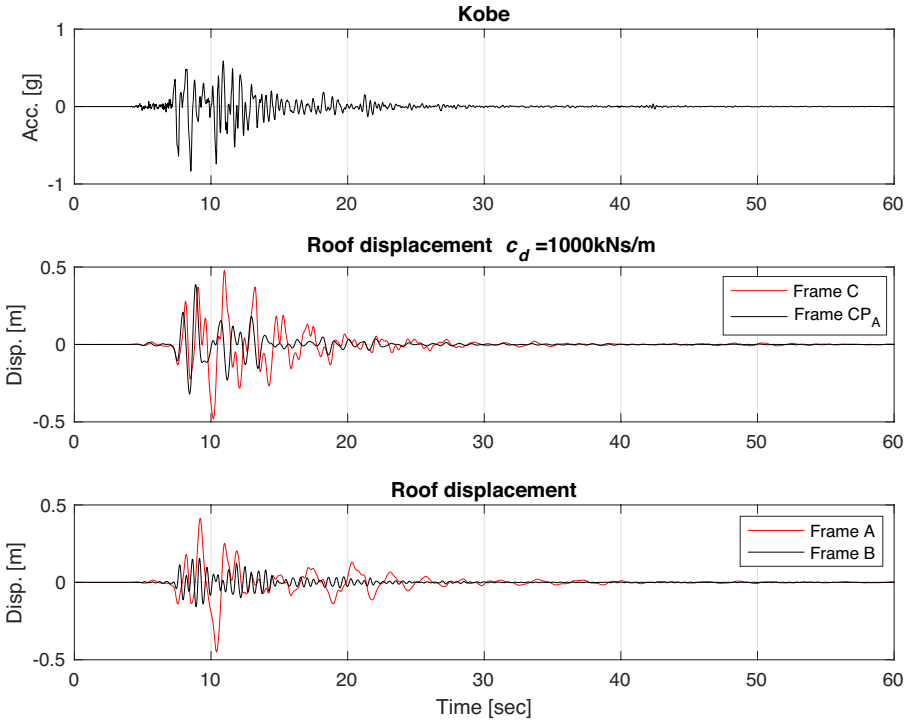

d *Kobe Earthquake*

FIG. 9 Roof level displacement time histories (VF dampers)

Figure 9 shows the dynamic responses of the frames at roof level under the four selected ground motions. The figures are arranged with ground motion plots to facilitate easy comparison. Frame-C refers to the roof displacement of the control frame (see Figure 3) without dampers. Frame CP_A

refers to the roof displacements of Frame-A (see Figure 3) when it is coupled with Frame-B with linear VF dampers. It is clear that by introducing a seismic gap and coupling two frames with VF dampers, displacement responses are significantly reduced under all simulated ground motions. The dynamic responses are much smaller than those of traditional construction (Frame-C). For comparison, the responses of Frame-A and B, which vibrate individually without any connection, is also shown. Due its small seismic mass and high lateral stiffness, Frame-B experiences very small displacements, while the opposite occurs to Frame-A. The viscous dampers' damping coefficient c_d is determined through a parametric study presented in the next section. Its value is within the range commercially available.

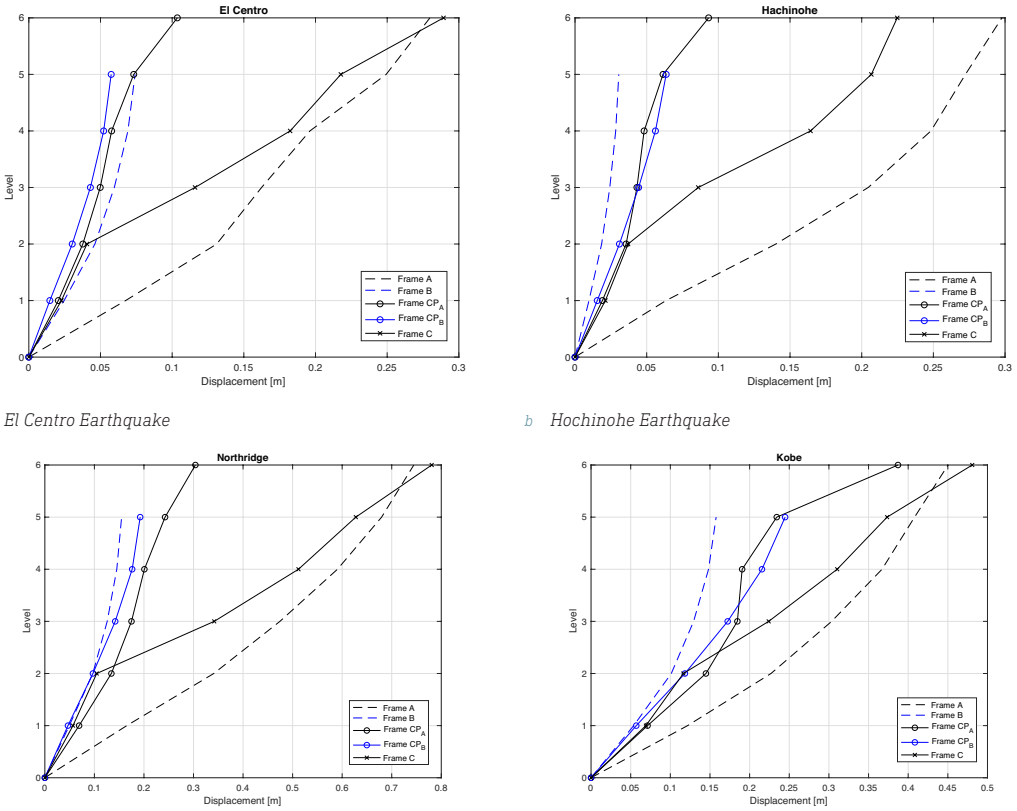

a *El Centro Earthquake*

b *Hochinohe Earthquake*

c *Northridge Earthquake*

d *Kobe Earthquake*

FIG. 10 Absolute maximum storey displacements (VF dampers)

Figure 10 shows the absolute maximum level displacements under the four selected ground motions. Frame CP_A and CP_B refer to the A and B side of the coupled frame, respectively. Displacement of CP_B also represents the lateral displacement experienced by the masonry façade. Storey displacement of Frame-C is compared. In all simulated ground motions, it is clear that Frame CP_A and CP_B undergo much smaller displacements due to the introduction of viscous dampers. The elastic limit of the masonry façade is also indicated in the plots, and it can be observed that under the El Centro and Hachinohe earthquakes (far-field records), displacement demand on CP_B is below the elastic limit. Thus, the masonry façade may be assumed to be undamaged. On the other hand, under the strong motion of Northridge and Kobe earthquakes (near-field records), the displacements of CP_B exceed such limits and the façade wall is expected to have been damaged.

In Figure 10, the absolute displacements of Frame-A and Frame-B, which vibrate individually without coupling, are also shown. Frame-B experienced the smallest amount of displacement due to its high stiffness and small mass, while Frame-A experiences the largest displacements. Generally, Frame CP_A and CP_B and C vibrate within those of A and B.

3.4 PARAMETRIC STUDY OF VF DAMPER PROPERTY

The choice of damper property will depend on structural dynamic characteristics, size of seismic gap, as well as the input ground motion. It is difficult to realise the suitable damper property by the height or mass of the new construction. Without a complex optimisation procedure, the suitable damping coefficient c_d of the dampers can be determined through a simple sensitivity study. For the above numerical examples, a range of c_d values are used in the time-domain analysis using the El Centro and Northridge ground motions. k_d is assumed as zero. Structural performance is evaluated using the following evaluation criteria suggested by Ohtori et al., (2004).

$$J_1 = \max\left\{\frac{\max t,i\dfrac{|d_i(t)|}{h_i}}{g\max}\right\} \tag{16}$$

$$J_2 = \max\left\{\frac{\max t,i|\ddot{x}_{ai}(t)|}{\ddot{x}\underset{a}{\max}}\right\} \tag{17}$$

$$J_3 = \max\left\{\frac{\max t,i\left|\sum_i m_i \ddot{x}_{ai}(t)\right|}{F\underset{b}{\max}}\right\} \tag{18}$$

J_1 is a criterion measuring the peak inter-storey drift ratios, J_2 measures structural level accelerations and J_3 measures base shear ratios. $d_i(t)$ is the inter-storey drift of the i^{th} storey over the time history. h_i is the height of each associated storeys. $\delta_{\max}$ is the maximum inter-storey drift ratio of the uncontrolled structure; in the context of this article it is the maximum inter-storey drift of Frame-C. $\ddot{x}_{ai}(t)$ is absolute acceleration of the i^{th} story and $\ddot{x}_a^{\max}$ is the absolute acceleration on any level of Frame-C; m_i is the seismic mass of the i^{th} storey and $F_b^{\max}$ is the maximum base shear experienced by Frame-C at any instance during the ground excitation.

Figure 11 shows the evaluation parameters J_1, J_2, and J_3 in response to a wide range of c_d, under the El Centro and Northridge excitations. At $c_d = 1000kNs/m$, it appears that all evaluation parameters reach optimal values approximately. As shown in the figure, the evaluation for inter-storey drift J_1 show improvements for all values of c_d. It is a clear indication that by introducing a seismic gap and placing dampers between adjacent levels is effective in controlling inter-storey drifts. On the other hand, J_2 which evaluates the peak accelerations experienced on various levels of the building, improvements are shown only at values c_d within the range between $1x10^5$ and $2x10^6$ Ns/m. The result for J_3 varied in El Centro and Northridge excitations, but shows best performance with c_d is close to $1x10^6 Ns/m$. It should be noted that this c_d value is readily available in commercial VF dampers, such as the manufacturers discussed in Section 2.3.

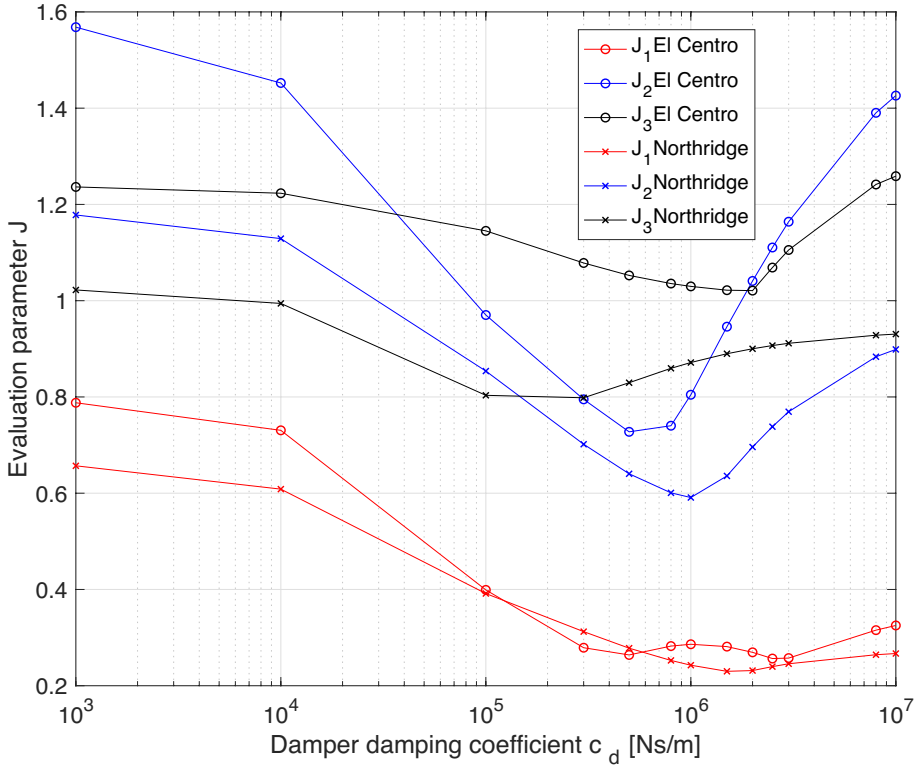

FIG. 11 Sensitivity study of VF damper coefficient

3.5 PERFORMANCE WITH FRICTION DAMPERS

The numerical analyses are now conducted with the VF dampers replaced by linear-motion friction dampers. Equations 11-15 are formulated in MATLAB. Frictional force f_d is set to 300kN and remains identical throughout the height of the building. The differential equations are solved by 4th order Runge-Kutta method (MATLAB command *ode45*). The numerical models are subjected to the same earthquake histories described previously. Displacement histories of the roof levels are graphically presented in Figure 12.

Effects of friction dampers are clear in all four simulated ground motions. Similar to the previous results of VF dampers, roof displacements are significantly controlled, as compared to the uncontrolled Frame-C. Figure 13 shows the absolute maximum level displacements under the four selected ground motions using friction dampers. Displacement responses of Frame-CP$_B$ may also be considered as the response of the masonry façade. Similar to the VF damper simulations, the response of Frame-CP$_B$ is below the elastic limit of the façade under the El Centro and Hachinohe earthquakes (far-field records), but exceed that under Northridge and Kobe earthquake (near-field records). The result indicates that the proposed structural form may mitigate seismic damages to the façade under El Centro and Hachinohe earthquakes, but unable to do so if the system is struck by Northridge or Kobe earthquakes. Similar observations were made when VF dampers were used in the previous section.

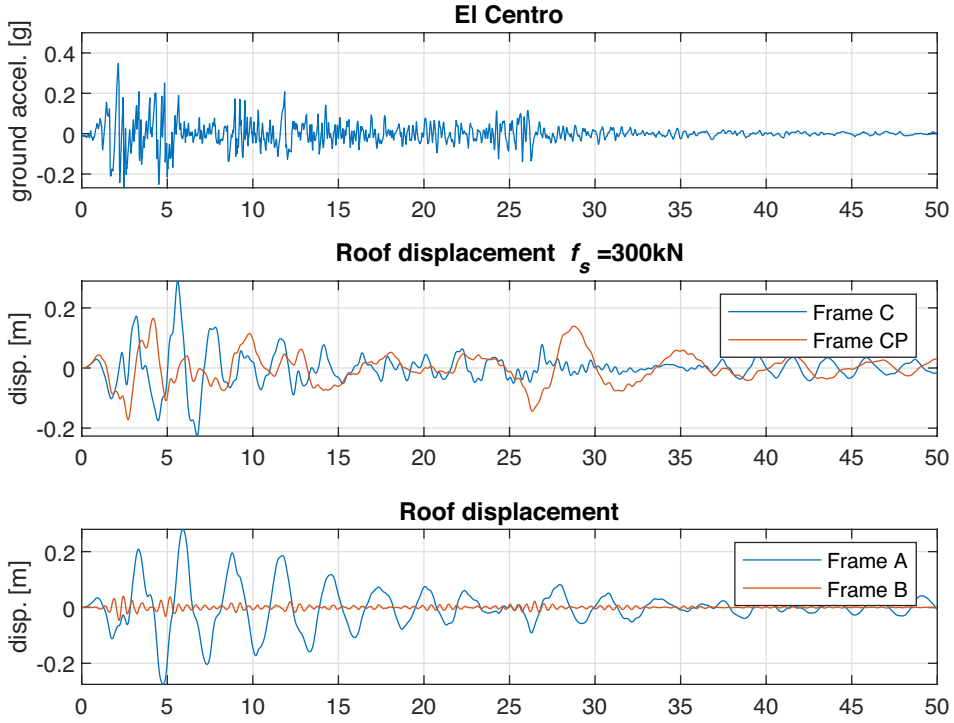

a *El Centro Earthquake*

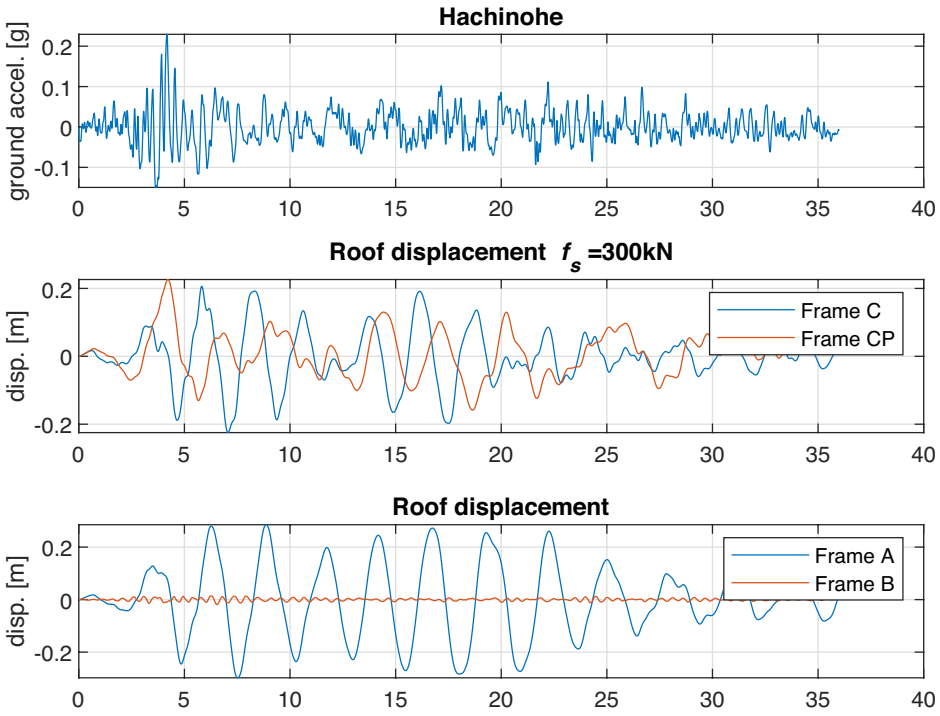

b *Hochinohe Earthquake*

FIG. 12 Roof level displacement time histories (friction dampers)

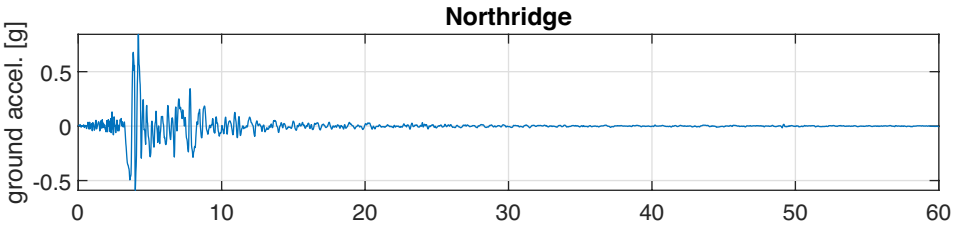

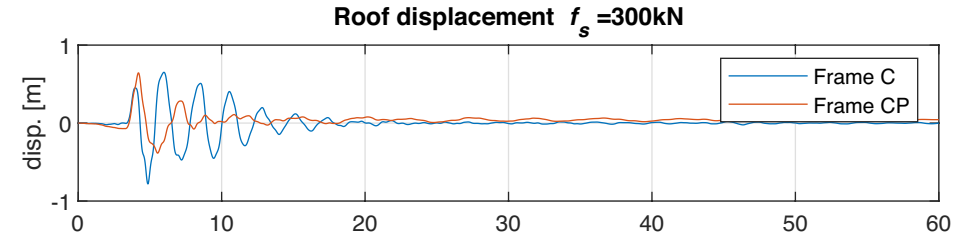

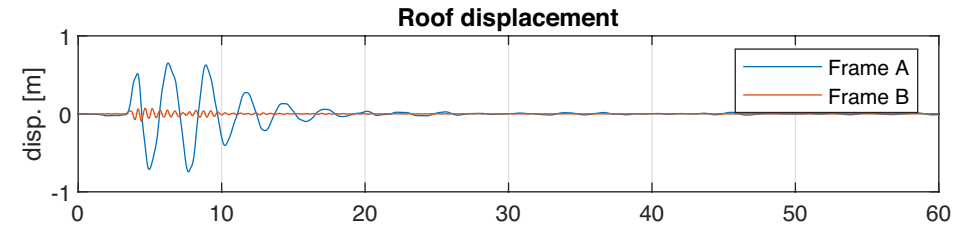

c *Northridge Earthquake*

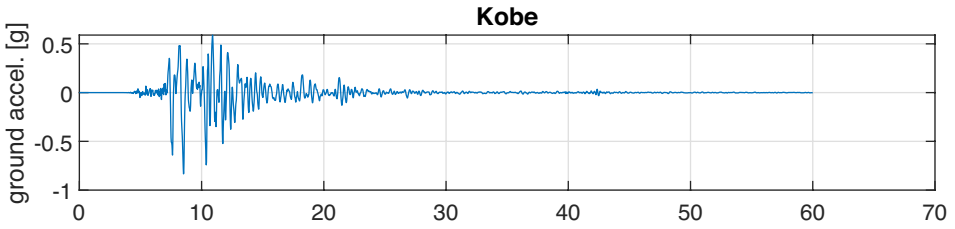

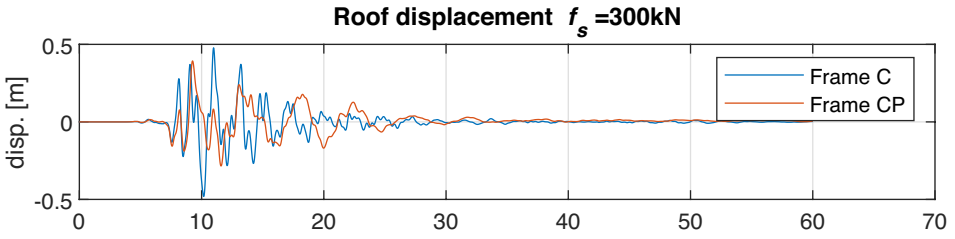

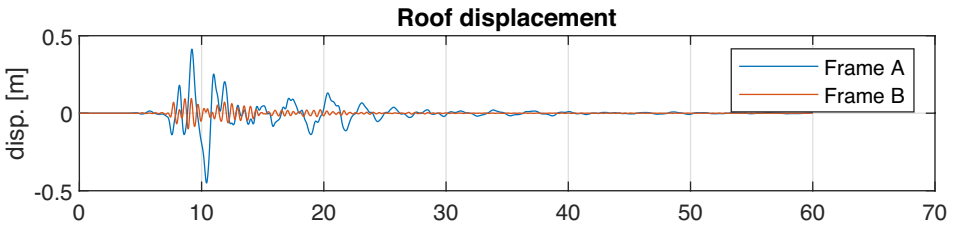

d *Kobe Earthquake*

FIG. 12 Roof level displacement time histories (friction dampers)

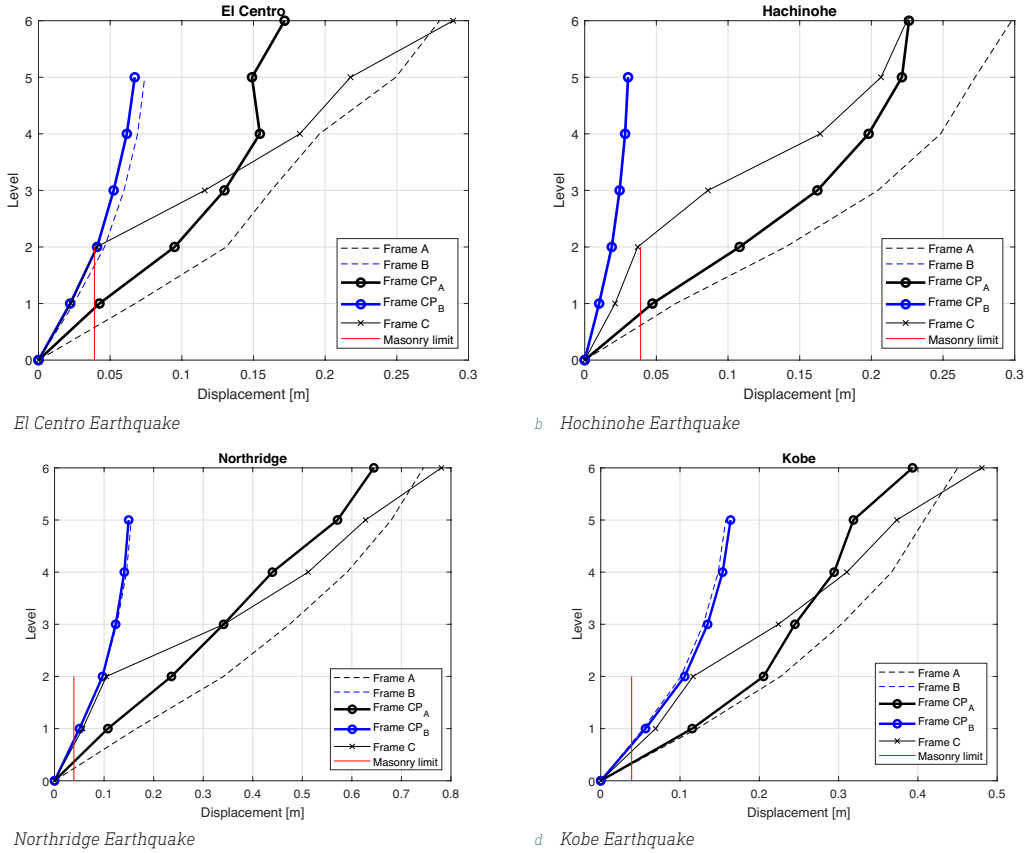

a *El Centro Earthquake*

b *Hochinohe Earthquake*

c *Northridge Earthquake*

d *Kobe Earthquake*

FIG. 13 Absolute maximum story displacements (friction dampers)

4 DISCUSSION ON PRACTICAL IMPLEMENTATION

Through a numerical example in Section 3, it was demonstrated that vibrational responses are suppressed by the proposed structural form, as compared to those of a traditional structural form without introduction of seismic gap and energy dissipating devices. In this section, several aspects of practical implementations are discussed.

4.1 PARTITIONING OF STRUCTURE

The proposed structural form relies on relative velocities (for VF dampers) or relative displacements (for friction dampers) of neighbouring floors to dissipate vibrational energies. Hence, it is essential to create two frames of very different vibrational characteristics (i.e. different vibrational periods). To avoid excessive displacement demand on the masonry façade, it is a clear choice that the façade is supported by a frame with small seismic mass and large lateral stiffness. It will ensure the façade will undergo minimal displacement responses under design ground motions. A seismically detailed reinforced concrete frame, shear wall, or a braced steel frame can be used. On the other hand, high displacement capacity must be designed in the frame of Frame-A. Seismically detailed reinforced concrete frame or steel moment-resisting-frames can be used.

4.2 SEISMIC GAP

Seismic gap – the width of seismic gap must be large enough to avoid the pounding of two frames under design excitations. The formulation described in Section 2 does not account for the impact forces that may occur if two frames are allow to pound on each other. Such impact force may have a detrimental effect on the masonry façade. The width of seismic gap can be conservatively estimated by summation of the absolute relative displacement of Frame-CP_A and Frame-CP_B. A large seismic gap, however, will require architectural treatment such as covering by panels. On the other hand, the seismic gap can be used as a space for vertical transportation of building services.

4.3 MASONRY FAÇADE

Elastic limit of masonry façade – it is not always possible to prevent damage to the brittle masonry façade under strong ground motions. As illustrated in the numerical examples, under the Northridge and Kobe earthquakes, Frame-B (hence the seismic demand to façade) is beyond the façade's elastic limit for both VF dampers and friction dampers. If such strong earthquake motions are expected in the building design life, it is necessary to retrofit the masonry façade to enhance its displacement capacity. Retrofit measures such as addition of steel strips, post-tensioning, or fibre-reinforced polymers discussed in Section 1.2 may be required. Anchorage of masonry façade to the new construction also requires proper consideration of seismic effects.

4.4 CHOICE OF DAMPER TYPES, LOCATIONS, AND QUANTITIES

Both VF and friction dampers are proven to be effective in suppressing structural vibration by dissipating a portion of input earthquake energies (Soong & Costantinou, 2014). Both types of damper are commercially available and design software is also readily available. Selection of the damper type is often dependent on cost, design, and maintenance experience.

TABLE 3 Comparison between VF and friction dampers

	VF DAMPERS	FRICTION DAMPERS
Principles	Velocity dependent	Displacement dependent
Damping force	Variable depending on travel velocity	Constant
Temperature	Damper properties are temperature dependent	Insensitive to temperature
Wind effects	Always dissipating energy including wind effects at serviceability limit state	Slip load must be larger than service load, i.e. dampers are not activated under service wind effects
Supporting members	Supporting members exert different forces in different earthquakes and must be designed for maximum credible earthquake (MCE) forces.	Supporting members exert constant forces regardless of earthquake characteristics.
Durability	Durability issues of seals which may lead to fluid leakage Change of damping force due to polymerization of silicone oil.	Frictional force may change due to corrosion and / or creep
Repair /Replacement	Complete replacement	Parts of damper can be replaced

Table 3 provides a brief comparison between the two types of dampers discussed in this work. On the other hand, dampers should be positioned such that the axial force exerted can be efficiently distributed to the lateral-load-resisting system of both frames. This can be achieved by locating the dampers close to the floor diaphragm. The quantity of dampers is dictated by seismic forces and is case-dependent, i.e. it depends on design earthquakes or maximum considered event (MCE), seismic masses, lateral stiffness and damping of frames, etc. However, using more dampers to distribute seismic forces more evenly will alleviate concentration of forces in certain structural members, but at a higher cost on procurement of dampers.

Finally, it should be noted that the results presented in Section 3 are specific to the characteristics of evaluation model and the select input earthquakes.

5 CONCLUSIONS

Continual population growth in major cities, increasing land values, and renewal of the aging urban areas have increased pressure to redevelop heritage buildings. Façadism is a popular trend in contemporary architecture. Façadism typically involves retaining street-elevation façades of a heritage building, while the remaining building is demolished and a new one is constructed behind the façade according to modern architecture and construction requirements. It is a form of compromise between conservation of heritage and redevelopments. Due to historical reasons, heritage façades are usually made of unreinforced stone or brick masonry with low ductility, and they are seismically vulnerable. While most existing studies focus on seismic assessment, strengthen of masonry structures, and improvement of connection design between façades and the main structure, this study takes a different approach by attempting to reduce seismic displacement demand on retained masonry façade in facadism constructions. In this work, we propose a new structural form to mitigate the seismic risks. Its principles are based on vibrations of two structural forms with different vibrational characteristics, and passive energy dissipation. The new building is partitioned into two frames by a seismic gap. The retained masonry façade is immediately supported by a frame with a lower natural vibration period, while the remainder of the new construction is built using a frame with a longer vibration period. Between each adjacent level, supplemental energy devices such as viscous fluid (VF) dampers or friction dampers are incorporated. Using two different vibrational characteristics of frames, the dampers absorb part of the input energy, thus suppressing vibration of the entire structural form. In particular, the displacement demand for the façade can be controlled and damages can be prevented. For VF dampers, damper forces are related to the velocities of adjacent floors on the same level, while for friction dampers, damper forces are dependent on normal forces applied to the damper, which can be adjusted according to requirements. In this paper the governing equations of motions of the proposed structural form are presented, first with VF dampers, followed by friction dampers. Through numerical examples, it was demonstrated that the proposed structural form is effective in reducing earthquake responses and represents a feasible solution to mitigating seismic risks in similar construction. With VF and friction dampers widely available commercially, the study represents a practical and feasible alternative method in façadism constructions. Finally, reviews of literature revealed that studies into seismic-risk mitigation of facadism construction is rare. Further research efforts in passive, semi-active and active vibration control, as well as large-scale shake table tests will be invaluable in safeguarding many of these constructions around the world.

References

Abdulla, K., Cunningham, L., & Gillie, M. (2017). Simulating masonry wall behaviour using a simplified micro-model approach. *Engineering Structures, 151*, 349.

Alshawa, O., Sorrentino, L., & Liberatore, D. (2017). Simulation Of Shake Table Tests on Out-of-Plane Masonry Buildings. Part (II): Combined Finite-Discrete Elements. *International Journal of Architectural Heritage, 11*(1), 79-93. doi:10.1080/15583058.2016.1237588

Bedon, C. & Amadio, C. (2017). Enhancement of the seismic performance of multi-storey buildings by means of dissipative glazing curtain walls. *Engineering Structures, 152*, 320-334. doi:10.1016/j.engstruct.2017.09.028

Bedon, C. & Amadio, C. (2018). Numerical assessment of vibration control systems for multi-hazard design and mitigation of glass curtain walls. *Journal of Building Engineering, 15*, 1-13. doi:10.1016/j.jobe.2017.11.004

Bhaskararao, A.V. & Jangid, R.S. (2006). Seismic analysis of structures connected with friction dampers. *Engineering Structures, 28*(5), 690-703. doi:10.1016/j.engstruct.2005.09.020

Bullen, P.A. & Love, P.E.D. (2011). Adaptive reuse of heritage buildings. *Structural Survey, 29*(5), 411-421. doi:10.1108/02630801111182439

Candeias, P.X., Campos Costa, A., Mendes, N., Costa, A.A., & Lourenço, P.B. (2017). Experimental Assessment of the Out-of-Plane Performance of Masonry Buildings Through Shaking Table Tests. *International Journal of Architectural Heritage, 11*(1), 31-58. doi:10.1080/15583058.2016.1238975

Chácara, C., Mendes, N., & Lourenço, P.B. (2017). Simulation of Shake Table Tests on Out-of-Plane Masonry Buildings. Part (IV): Macro and Micro FEM Based Approaches. *International Journal of Architectural Heritage, 11*(1), 103-116. doi:10.1080/15583058.2016.1238972

Chan, R.W.K. & Hu, B. (2016). Numerical and experimental investigation into friction devices installed between concrete columns and steel beams. In C. Z. Hong Hao (Ed.). Taylor and Francis Group (United Kingdom).

Chang, C.-M., Strano, S., & Terzo, M. (2016). Modelling of Hysteresis in Vibration Control Systems by means of the Bouc-Wen Model. *Shock and Vibration, 2016*. doi:10.1155/2016/3424191

Constantinou, M., Mokha, A., & Reinhorn, A. (1990). Teflon Bearings in Base Isolation II: Modeling. *Journal of Structural Engineering, 116*(2), 455-474. doi:10.1061/(asce)0733-9445(1990)116:2(455)

Constantinou, M.C. & Symans, M.D. (1993). Experimental study of seismic response of buildings with supplemental fluid dampers. *Journal of Structural Design of Tall Buildings, 2*(2), 93-132.

Dal Lago, B., Negro, P., & Dal Lago, A. (2018). Seismic design and performance of dry-assembled precast structures with adaptable joints. *Soil dynamics and earthquake engineering (1984), 106*, 182-195. doi:10.1016/j.soildyn.2017.12.016

Darley, G. (2015). Facadism. *Architects' Journal, 241*(7), 70-71.

De Domenico, D., Ricciardi, G., & Takewaki, I. (2019). Design strategies of viscous dampers for seismic protection of building structures: A review. *Soil Dynamics and Earthquake Engineering, 118*, 144-165. doi:10.1016/j.soildyn.2018.12.024

Derakhshan, H., Nakamura, Y., Ingham, J.M., & Griffith, M.C. (2017). Simulation of Shake Table Tests on Out-of-Plane Masonry Buildings. Part (I): Displacement-based Approach Using Simple Failure Mechanisms. *International Journal of Architectural Heritage, 11*(1), 72-78. doi:10.1080/15583058.2016.1237590

Ferreira, T., Vicente, R., & Varum, H. (2010). *Seismic vulnerability assessment of masonry façade walls*. Paper presented at the 14th European Conference on Earthquake Engineering, Ohrid, Republic of Macedonia.

Figueiredo, A., Varum, H., Costa, A., Silveira, D., & Oliveira, C. (2013). Seismic retrofitting solution of an adobe masonry wall. *Materials and Structures, 46*(1), 203-219. doi:10.1617/s11527-012-9895-1

Griffith, M.C. & Vaculik, J. (2007). Out-of-Plane Flexural Strength of Unreinforced Clay Brick Masonry Walls. *TMS Journal, 25*(1), 53-68.

Grigorian, C.E., Yang, T.S., & Popov, E.P. (1993). Slotted Bolted Connection Energy Dissipators. *Earthquake Spectra, 9*(3), 491-504. doi:10.1193/1.1585726

Habibi, A., Chan, R.W.K., & Albermani, F. (2013). Energy-based design method for seismic retrofitting with passive energy dissipation systems. *Engineering Structures, 46*, 77-86.

IIT Enidine Inc. Viscous dampers / Seismic dampers. https://www.itt-infrastructure.com/en-US/Products/Viscous-Dampers/

Ingham, J. & Griffith, M. (2010). Performance of Unreinforced Masonry Buildings During the 2010 Darfield (Christchurch, Nz) Earthquake. *Australian Journal of Structural Engineering, 11*(3), 207-224. doi:10.1080/13287982.2010.11465067

Ingham, J.M., Moon, M., & Griffith, M.C. (2011). *Performance of Masonry Buildings in the 2010/2011 Canterbury Earthquake Swarm and Implications for Australian Cities*. Paper presented at the Australian Earthquake Engineering Society 2011 Conference, Barossa Valley, South Australia.

Mariangela De, V., Antonio, M., Antonio, S., & Alessio, M. (2018). Seismic Retrofit Measures for Masonry Walls of Historical Buildings, from an Energy Saving Perspective. *Sustainability, 10*(4), 984. doi:10.3390/su10040984

Moës, N., Dolbow, J., & Belytschko, T. (1999). A finite element method for crack growth without remeshing. *International Journal for Numerical Methods in Engineering, 46*(1), 131-150. doi:10.1002/(SICI)1097-0207(19990910)46:1<131::AID-NME726>3.0.CO;2-J

Mualla, I.H., Jakupsson, E.D., & Nielsen, L.O. (2010). *Structural Behavior of 5000kN Damper*. Paper presented at the 14th European conference on earthquake engineering, Ohrid, North Macedonia.

Nakamura, Y. & Okada, K. (2019). Review on seismic isolation and response control methods of buildings in Japan. *Geoenvironmental disasters, 6*(1), 1-10. doi:10.1186/s40677-019-0123-y

Negro, P. & Lamperti Tornaghi, M. (2017). Seismic response of precast structures with vertical cladding panels: The SAFECLADDING experimental campaign. *Engineering Structures, 132*, 205-228. doi:10.1016/j.engstruct.2016.11.020

Ohtori, Y., Christenson, R.E., Spencer, B.F., Jr., & Dyke, S.J. (2004). Benchmark control problems for seismically excited nonlinear buildings. *Journal of Engineering Mechanics, 130*(4), 366. doi:10.1061/(ASCE)0733-9399(2004)130:4(366)

Reinhorn, A.M. & Constantinou, M.C. (1995). *Experimental and Analytical Investigation of Seismic Retrofit of Structures with Supplemental Damping, Part 1: Fluid Viscous Damping Devices*. Retrieved from

Reitherman, R. & Perry, S.C. (2009). *Unreinforced Masonry Buildings and Earthquakes*.

Rihal, S.S. (1988). *Seismic behavior and design of precast façades/claddings & connections on low/medium-rise buildings*. Retrieved from

Senaldi, I., Magenes, G., & Ingham, J.M. (2014). Damage Assessment of Unreinforced Stone Masonry Buildings After the 2010-2011 Canterbury Earthquakes. *International Journal of Architectural Heritage*. doi:10.1080/15583058.2013.840688

Solarino, F., Oliveira, D.V., & Giresini, L. (2019). Wall-to-horizontal diaphragm connections in historical buildings: A state-of-the-art review. *Engineering Structures, 199*, 109559. doi:10.1016/j.engstruct.2019.109559

Soltanzadeh, G., Osman, H., Vafaei, M., & Vahed, Y. (2018). Seismic retrofit of masonry wall infilled RC frames through external post-tensioning. *Official Publication of the European Association for Earthquake Engineering, 16*(3), 1487-1510. doi:10.1007/s10518-017-0241-4

Soong, T.T. & Costantinou, M.C. (2014). *Passive and active structural vibration control in civil engineering* (Vol. 345). Springer.

Spencer, B.F., Jr., Dyke, S.J., Sain, M.K., & Carlson, J.D. (1997). Phenomenological model for magnetorheological dampers. *Journal of Engineering Mechanics, 123*(3), 230. doi:10.1061/(ASCE)0733-9399(1997)123:3(230)

Symans, M., Charney, F., Whittaker, A., Constantinou, M., Kircher, C., Johnson, M., & McNamara, R. (2008). Energy Dissipation Systems for Seismic Applications: Current Practice and Recent Developments. *Journal of Structural Engineering, 134*(1), 3-21. doi:doi:10.1061/(ASCE)0733-9445(2008)134:1(3)

Taghdi, M., Bruneau, M., & Saatcioglu, M. (2000). Seismic retrofitting of low-rise masonry and concrete walls using steel strips. *Journal of Structural Engineering, 126*(9), 1017-1025. doi:10.1061/(ASCE)0733-9445(2000)126:9(1017)

Tam, V.W.T., Le, K.N., & Wang, J.Y. (2018). Cost Implication of Implementing External Façade Systems for Commercial Buildings. *Sustainability, 10*(6), 1917. doi:10.3390/su10061917

Taylor Devices Inc. Fluid Viscous Dampers. https://www.taylordevices.com/products/fluid-viscous-dampers/

Tiziana, B. & Daniele, E. (2018). Seismic and Energy Retrofit of the Historic Urban Fabric of Enna (Italy). *Sustainability, 10*(4), 1138. doi:10.3390/su10041138

Triantafillou, T.C. (2001). Seismic retrofitting of structures with fibre-reinforced polymers. *Progress in Structural Engineering and Materials, 3*(1), 57-65. doi:10.1002/pse.61

Wang, S.J., Lin, W.C., & Yang, C.Y. (2017). *Recent Progress in Taiwan on Seismic Isolation, Energy Dissipation, and Active Vibration Control*. Paper presented at the 2017 New Zealand Society Earthquake Engineering Conference.

Wen, Y.K. (1976). Method for Random Vibration of Hysteretic Systems. *Journal of the Engineering Mechanics Division-Asce, 102*(2), 249-263.

Xu, Y., He, Q., & Ko, J. (1999). Dynamic response of damper- connected adjacent buildings under earthquake excitation. *21*(2), 135-148.

Zhu, X. & Lu, X. (2011). Parametric Identification of Bouc-Wen Model and Its Application in Mild Steel Damper Modeling. *Procedia Engineering, 14*(C), 318-324. doi:10.1016/j.proeng.2011.07.039